Exploring NSM technique for torsional strengthening of tubular type RC structures

Chandan C. Gowda, Joaquim A O Barros

ISISE, Department of Civil Engineering,
University of Minho,
Campus de Azurém, Guimarães (4800 019), Portugal

Abstract

The present paper explores, by advanced numerical simulations, the potentialities of the Near Surface Mounted (NSM) technique for the torsional strengthening of thin walled tubular type reinforced concrete (RC) elements. According to this technique, fibre reinforced polymer (FRP) laminates are introduced into thin grooves opened on the concrete cover of the RC elements. A 3D multidirectional smeared crack model available in FEMIX computer code is used for the numerical simulations, and its predictive performance for capturing the behaviour of this type of elements was assessed by simulating experimental tests available in the literature. This model was then used to determine the influence of the variation of longitudinal reinforcement, transverse reinforcement and the concrete compressive strength on the torsional behaviour of thin walled tubular RC elements, with the focus on torque-angle of rotation response. The effect of the variation of the FRP's modulus of elasticity is also investigated. The results allow to conclude that the proposed NSM strengthening technique is effective in increasing the stiffness and the load carrying capacity, as well as in arresting crack propagation of the strengthened tubular RC elements.

1 Introduction

Strengthening of concrete structures is a field of civil engineering where a significant research investment is being done due to the huge market associated to the rehabilitation of the built environment. Structural strengthening is, generally, justified by the following reasons: to meet the design requisites imposed by new codes; fix the damages due to deficient design and/or construction, degradation of constituent materials, damages due to extreme events or loading conditions not considered in the design process, change in the building usage, etc.

Relevant research activities in the structural rehabilitation are being carried out using fibre reinforced polymer (FRP) systems due to their advantages when compared to the solutions based on conventional materials like RC and steel plates and profiles, namely, their immunity to corrosion, higher (stiffness & strength)/self-weight ratio, easiness of application, and small changes in the architectural attributes of the building to be strengthened. FRPs are being applied mainly according to the externally bonded reinforcement (EBR) and the near surface mounted (NSM) techniques. In EBR, the FRP materials, in the form of laminates or sheets, are applied on the external surfaces, whereas in the NSM technique laminates or rods are introduced into thin grooves opened on concrete cover of the RC elements. In both techniques FRPs are bonded to the concrete substrate by using structural adhesives, the most current is an epoxy.

Some RC bridges are formed by tubular type structural elements, and increasing their torsional stiffness and capacity is required in some cases, which is the main motivation of the present research. However, torsional strengthening of thin walled tubular RC structures using EBR or NSM is a field where very little or limited research is available ((Panchacharam and Belarbi 2002), (Deifalla and Ghobarah 2005), (Hii and Al-Mahaidi 2006), (Jing, Raongjant, and Li 2007), (Al-Mahaidi and Hii 2007), (Chalioris 2007), (Chalioris 2007), (Chalioris and Karayannis 2009), (Deifalla and Ghobarah 2010), (Deifalla, Awad, and Elgarhy 2013)). According to the knowledge of the authors of the present work, no research data is available on the NSM torsional strengthening of thin walled tubular structural elements, in spite of the recognized efficiency of NSM for the shear strengthening of RC beams (Dias and Barros 2013).

Near surface mounted (NSM) technique possess many advantages over the EBR method, like the ease of application, more effective utilization of the FRP materials, better protection against acts of vandalism and fire. Since this technique seems to be not yet applied for the torsional strengthening of

tubular RC structures, its potentialities will be investigated in this work by performing numerical analysis with a computer program capable of simulating the relevant behaviour of the constituent materials of this type of structures. After verifying the good predictive performance of the constitutive models to be adopted, by simulating an experimental torsional test with a RC beam, a parametric study was carried out for assessing the influence of the following parameters on the torsional strengthening efficiency when using NSM technique: longitudinal reinforcement ratio, transverse reinforcement ratio, concrete compressive strength, different NSM shear strengthening configurations.

2 Assessment of the predictive performance of a 3D constitutive model for the simulation of the nonlinear behaviour of RC elements strengthened in torsion

For simulating numerically the behaviour of reinforced concrete (RC) elements subjected to torsional loading conditions, the 3D multidirectional fixed smeared crack model described in (Gouveia 2011), and available in FEMIX computer program, will be used. Its predictive performance in the simulation of this type of structures was firstly assessed by simulating the reference box-section beam experimentally tested by (Al-Mahaidi and Hii 2007), whose details are presented in Fig. 1. Table 1 presents the values of the model parameters adopted for the concrete constitutive model. Solid finite elements of 8 nodes, with Gauss-Legendre (GL) integration scheme of 2×2×2 integration points (IP) is adopted, with a convergence criteria in energy limited to the tolerance of 1×10^{-3}. The physical meaning of the variables in Table 1 is presented in Gouveia 2011. The crack propagation in mode I is simulated by a trilinear diagram, adopting a fracture energy ($G_{f,I}$) of 0.08 N/mm according to the EuroCode 2 (2004) recommendations. For modelling the crack propagation in modes II and III, a bilinear diagram was adopted with an equal fracture energy of 0.3 N/mm in both the modes, according to (Baghi et al. 2016, Breveglieri 2015). The transverse reinforcement is made up of 6 mm diameter steel bars with modulus of elasticity (E_s) of 213.44 GPa and yield strength of 426.5 MPa, while the 10 mm longitudinal bars had a E_s of 207.05 GPa and a yield strength of 398.2 MPa. These bars were modelled with embedded cables of 2 nodes, of 2 GL IP, assuming they are perfectly bonded to the corresponding concrete mother elements. Previous research demonstrates that fracture of concrete surrounding the NSM-FRP is the governing failure mode during the pullout process of this composite material crossed by a crack (shear or flexural nature) and debonding is only significant when the bond transfer length is less than a critical value. Taking this into consideration and aiming not to introduce unnecessary complexities in the numerical simulations, perfect bond was assumed between the laminates and the concrete.

Table 1 Values of the parameters for the concrete constitutive model.

Description	Values for the simulation of Al-Mahaidi and Hii 2007)	Values for the parametric analysis
Poisson's ratio (ν_c)	0.15	0.15
Young's modulus (E_c)	35000 MPa	29000 MPa
Compressive strength (f_c)	48.90 MPa	25 MPa
Trilinear tensile softening diagram	$f_{ct} = 3\ MPa;\ G_{f,I} = 0.08\frac{N}{mm};\ \xi_1 = 0.01;\ \alpha_1 = 0.5;\ \xi_2 = 0.3;\ \alpha_2 = 0.2$	$f_{ct} = 2\ MPa;\ G_{f,I} = 0.07\frac{N}{mm};\ \xi_1 = 0.01;\ \alpha_1 = 0.5;\ \xi_2 = 0.3;\ \alpha_2 = 0.2$
Parameters for defining the softening crack shear stress-shear strain diagram of concrete in the tension-stiffening	$\tau_{t,p}^{cr} = 2.0\ MPa;\ G_s = 0.3\frac{N}{mm};\ \beta = 0.025$	$\tau_{t,p}^{cr} = 2.0\ MPa;\ G_{f,II} = 0.07\frac{N}{mm};\ \beta = 0.10$
Crack bandwidth (l_b)	$\sqrt[3]{V_{I,P}}$ (Cube root of the volume of the integration point)	$\sqrt[3]{V_{I,P}}$ (Cube root of the volume of the integration point)
Threshold angle	$\alpha_{th} = 30^0$	$\alpha_{th} = 30^0$
Maximum number of cracks per integration point	2	2

The 3 degrees of freedom of all the nodes in one extremity surface were fixed, while in the node P of the other extremity, only the vertical degree of freedom was fixed (Fig. 1 (left)). Load is applied on a steel arm as shown in Fig. 1 (left) producing the torsional moment (M_t), and torsional angle (θ_t), was measured in section S (400 mm from loading point). The M_t-θ_t registered experimentally and obtained numerically are compared in Fig. 1 (right), where it is visible that the model is capable of simulating accurately the experimental response up to the loading stage when steel reinforcement started yielding, and due to convergence difficulties the simulations were interrupted at θ_t=1.94 degrees. The predictive performace of a fracture mechanics based model is demonstrated when it is capable of simulating with high accuracy the structural response during the stage of cracking process, which is the present case.

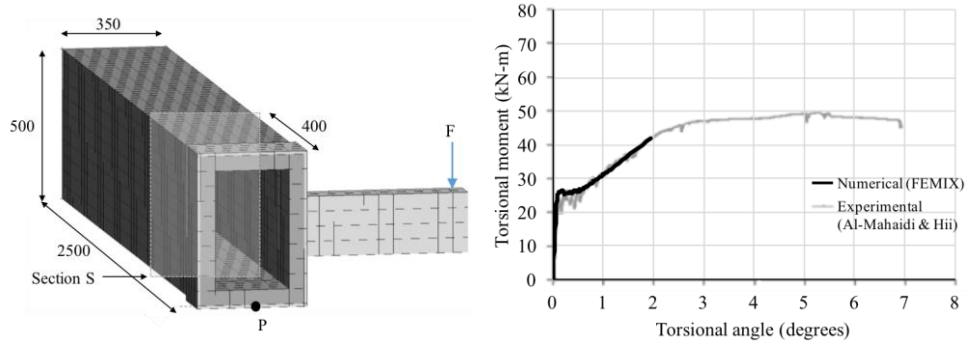

Fig. 1 Simulation of the reference beam experimentally tested by (Al-Mahaidi and Hii 2007): (left) details of the FEM model; (right) Numerical versus experimental simulations.

3 Parametric studies for assessing the influence of relevant parameters under the framework of torsional strengthening of RC elements

3.1 Geometry and data

The model beams have a geometry of 400 mm × 400 mm, with 100 mm wall thickness and an inner hollow tubular section of 200 mm × 200 mm. For the evaluation of the values of the parameters for the constitutive model the available experimental results were considered, and also taking into account the experience of the second author on the material nonlinear analysis of RC structures.The details about the longitudinal and transverse reinforcements are presented in Fig. 2 (left). One extremity of the beam has a steel section to apply the load, whereas the other extremity is fixed. These two sections are herein designated as loading and fixed sections, respectively. The extra transverse reinforcement applied at the extremities zones have the aim of avoiding local damage due to stress concentration caused by the loading and supporting apparatus always existing in experimental tests.

3.2 FEM attributes and material properties for the constitutive models

Concrete was simulated by solid elements of 8 nodes of 50 mm size length with GL 2×2×2 IP, while steel reinforcements and NSM CFRP laminates were modelled by embedded cables of 2 nodes with GL 2 IP. The load and support conditions is represented in Fig. 2 (right). In the third column of Table 1 the values of the model parameters adopted for the concrete is provided, while for steel reinforcements an elasticity modulus of 200 GPa and a yield stress of 400 MP was assumed, with a perfectly plastic behaviour beyond yield strain. A linear elastic isotropic behaviour was assumed for the CFRP laminates by using an elasticity modulus of 160 GPa, with abrupt rupture when attaining its tensile strength (2500 MPa). All the simulations were executed with a modified version of the Newton-Raphson iterative algorithm, where the stiffness matrix is updated only in the first iteration of each load increment, and using the arc-length facility by controlling the vertical displacement of the loading point. Energy convergence criterion with a tolerance of $1x10^{-3}$ was adopted.

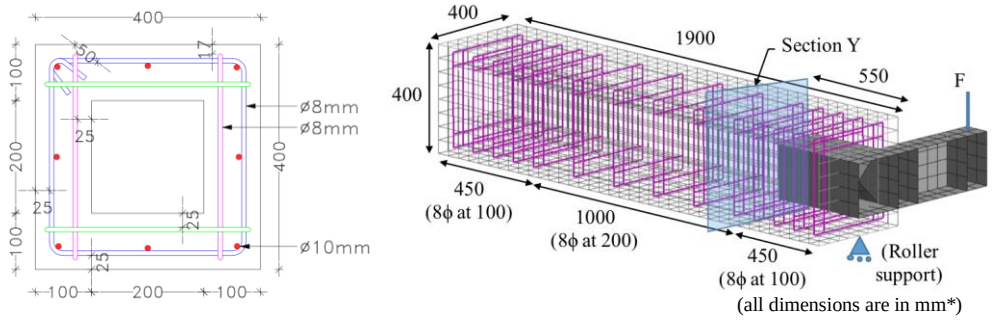

Fig. 2 Cross section (left), Finite element model of the beam (right)

The θ_t was measured at a distance of 550 mm from the loading section (100 mm from the extremity of the extra reinforced zone, Section Y), see Fig. 2 (right). The θ_t of this section has considered the in-plane degrees of freedom of all the nodes of the section and their distance to the geometric centre of the section.

3.3 Parametric analysis and discussion of the results

Parametric analysis is performed to study the influence of longitudinal and transverse reinforcements, as well as concrete compressive strength, on the torsional behaviour of tubular type RC structures (Table 2). The efficiency of NSM strengthening technique will be evaluated for the variation of reinforcement ratios on torsional behaviour. The results of the M_t-θ_t for these simulations are presented in Fig. 3, with markers indicating the yield initiation stage of transverse and longitudinal reinforcement, LY and TY, respectively. In the last two columns of Table 2 the maximum M_t and its corresponding θ_t is indicated, when the simulations were interrupted due to difficulties on assuring convergence caused by the formation of macro-cracks (fracture energy exhausted) bridged by reinforcements in the yielded stage.

Table 2 Details and relevant results of the parametric analysis

Beam's designation	Longitudinal reinforcement diameter (mm)	Transverse reinforcement diameter (mm)	Concrete strength class (MPa)	Maximum moment (kN·m)	Maximum angle of rotation (Degrees)
L8S8	8	8	C20/25	51.92	1.36
L10S8	10	8	C20/25	63.36	1.59
L12S8	12	8	C20/25	74.53	1.50
L10S6	10	6	C20/25	52.86	1.32
L10S10	10	10	C20/25	72.30	1.60
L10S8	10	8	C12/15	62.73	1.63
L10S8	10	8	C25/30	62.00	1.14
L10S8	10	8	C40/50	53.47	0.61

Since the concrete strength class was the same in the simulations of Fig. 3, the branch up to crack initiation was almost the same in these simulations, where it is quite evident the benefits in terms of torsional capacity when increasing the longitudinal reinforcement ratio, Fig. 3 (left), and the transverse reinforcement ratio, Fig. 3 (right). The increase of maximum torsional capacity is caused by the increase in the torsional stiffness, since the increase in these reinforcements reduce the number of cracks and limits the crack width propagation, promoting a larger beneficial effect of aggregate interlock in the cracked section. As expected, by increasing the ratio of these reinforcements has postponed their yield initiation for larger θ_t, mainly when transverse reinforcement ratio is increased.

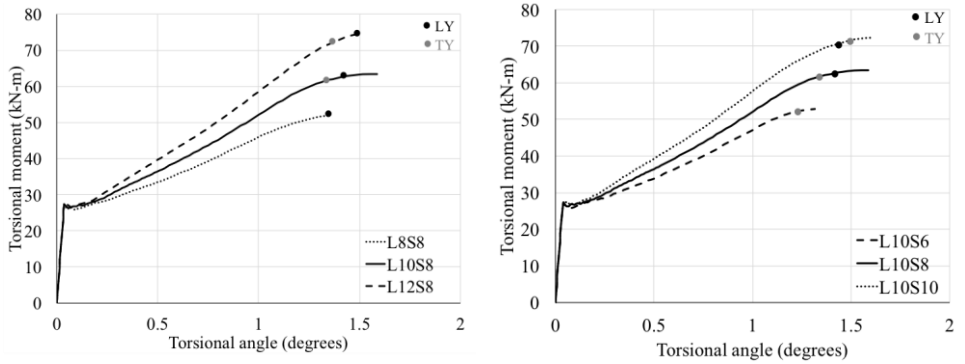

Fig. 3 Torque-angle of rotation curves for longitudinal reinforcement and transverse reinforcement variation

Fig. 4 presents the influence of the concrete strength class on the torsional capacity. The M_t at crack initiation has increased with the strength class, and since the longitudinal and transverse reinforcements were maintained the same in all the simulations, the stiffness of the torsional response after crack initiation was almost the same. In consequence, the torsional capacity is increased in load conditions corresponding to serviceability limit states, but the maximum torsional capacity (corresponding to the yield initiation of the reinforcements) is almost preserved the same at a θ_t that decreases with the increase of the strength class (loss of ductility). Due to difficulties in convergence, the simulation of L10S8_C40/50 has not attained the yield initiation of the reinforcements.

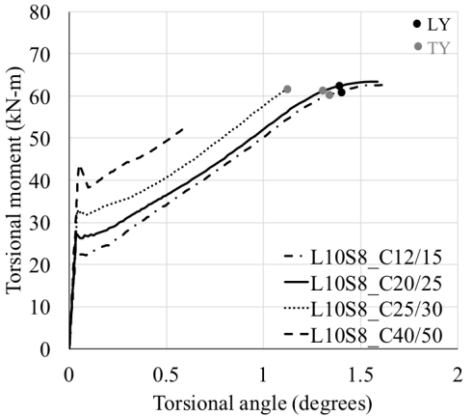

Fig. 4 Torque-angle of rotation for variation of concrete compressive strength

4 Exploring NSM strengthening configurations for thin walled RC structures

4.1 Strengthening configurations

Based on the results of the parametric analysis, four strengthening configurations are proposed for the beams, all based on the combination of transverse and longitudinal FRP laminates (of 10 × 1.4 mm^2 cross section), as shown in Fig. 5. The longitudinal laminates are placed first in the interior with a cover of 15 mm (centre of the laminate to the outer surface) and then the transverse laminates in the exterior, with a cover of 5 mm. The analysis is performed with all the other conditions being exactly the same as in the previous section. Two distances for the longitudinal (L_FRP: 134 and 80 mm) and transverse (T_FRP: 65 and 40 mm) FRP laminates were considered, disposed in the central test region of 1000 mm according to the following analysed configurations (Fig. 5). However only one set of transverse strengthening is presented, since presenting the full transverse strengthening in the central 1000 mm would be unclear. $\left[\rho_{l,eq} = \frac{A_{sl}}{(b_w d)} + \left(\frac{A_f E_f}{E_s}\frac{1}{b d_f}\right), \rho_{w,eq} = \frac{A_{sw}}{(b_w s_w)} + \left(\frac{A_f E_f}{E_s}\frac{1}{b s_f}\right)\right]$ ($\rho_{l,eq}$ = longitudinal equivalent reinf ratio, A_{sl}= longitudinal reinf area, b_w= width of web, d= effective depth, A_f= area of

FRP, E_f= mod of elasticity of FRP, E_s= mod of elasticity of steel, d_f = depth of FRP, $\rho_{w,eq}$= equivalent transverse reinf., A_{sw}= trasverse reinf area, s_w= transverse reinf spacing)

- FRP_1: L_FRP@134 mm on the four sides and T_FRP@65 mm between two stirrups (top left) ($\rho_{l,eq} = 0.232, \rho_{w,eq} = 1.036$)
- FRP_2: L_FRP@134 mm on the four sides and T_FRP@40 mm between two stirrups (top right) ($\rho_{l,eq} = 0.232, \rho_{w,eq} = 1.092$)
- FRP_3: L_FRP@80 mm on the four sides and T_FRP@65 mm between two stirrups (bottom left) ($\rho_{l,eq} = 0.246, \rho_{w,eq} = 1.036$)
- FRP_4: L_FRP@80 mm on the four sides and T_FRP@40 mm between two stirrups (bottom right). ($\rho_{l,eq} = 0.246, \rho_{w,eq} = 1.092$)

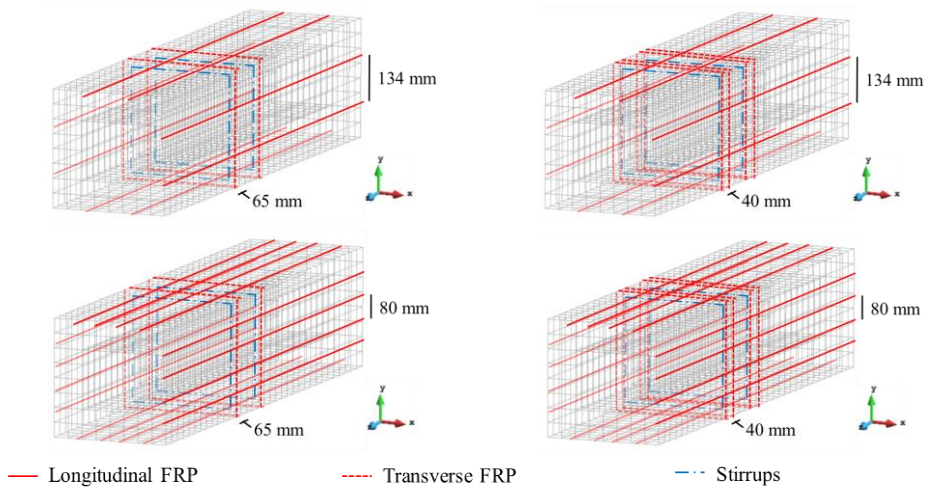

Fig. 5 Strengthening configurations: FRP_1 (Left top), FRP_2 (Right top), FRP_3 (Left bottom), FRP_4 (Right bottom)

4.2 Results

The M_t-θ_t for these strengthening configurations are represented in Fig. 6. At θ_t=1.67 degrees (when both the longitudinal and transverse reinforcement have already yielded) the increase in the torsional capacity of the FRP_1, FRP_2, FRP_3 and FRP_4 was, respectively, 7, 10, 12 and 15% when compared to the one of the reference L10S8 element ($\rho_{sl} = 0.218, \rho_{sw} = 0.980$). This means that the torsional capacity increases with both the longitudinal and transverse strengthening ratios. This figure also represents the relationship between maximum crack width (obtained as the product of the maximum crack normal strain to the crack band width of the corresponding IP) and θ_t for the four strengthening types. The crack width has reduced from 0.2 mm (ref beam) to 0.13 mm (FRP_4) thereby increasing the durability by limiting the crack width (35%).

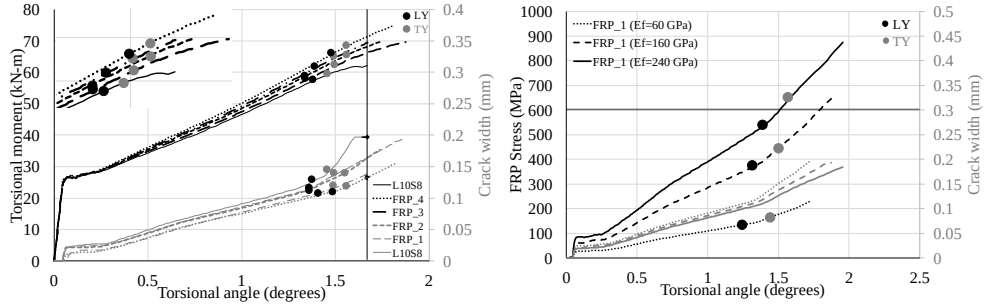

Fig. 6 Torque-angle of rotation for the proposed strengthened methods (left), Stress evolution in FRP for the variation of modulus of elasticity

For assessing the influence of the modulus of elasticity of the FRP laminates (E_f) on the torsional strengthening effectiveness, three values of E_f were selected (60, 160 and 240 GPa) by simulating the FRP_1 strengthening configuration. Fig. 6 (right) represents the maximum stress in the FRP versus the θ_t, where it is visible that by increasing E_f the maximum stress in the FRP increases and the yield initiation of the longitudinal and transverse reinforcement is postponed for larger θ_t. The configuration of the obtained line demonstrates the occurrence of three stages: 1) up to crack formation the FRP is not activated; 2) the FRP is significantly mobilized after crack initiation; 3) an accentuated gradient of maximum tensile stress occurs after yielding initiation of the longitudinal reinforcement. It is observed a significant reduction on the maximum crack width with the increase of E_f.

Since the application of NSM FRP systems seems to assure relatively small increase of torsional capacity for loading conditions corresponding to the SLS conditions, the application of the FRP_1 strengthening configuration with a prestress level of 50% of the FRP ultimate tensile capacity was simulated for both longitudinal and transverse FRP laminates. The M_t-θ_t relationship for the passive and prestress situations are compared in Fig. 7 (left). The benefits of applying the FRP with a certain prestress level is quite evident, by increasing significantly the torsional capacity for SLS conditions, postponing the yield initiation of the reinforcements and decreasing the maximum crack width. The relationship between the crack width and θ_t is also shown in Fig. 7 (left). By taking the advantage of the prestress that can be applied to FRPs and adopting an innovative type of NSM CFRP laminate recently developed by the second author (Rezazadeh et al. 2015), a new strengthening NSM-based active technique is aimed to be developed for the shear and torsional strengthening of tubular type bridge sections, as shown in Fig. 7 (right).

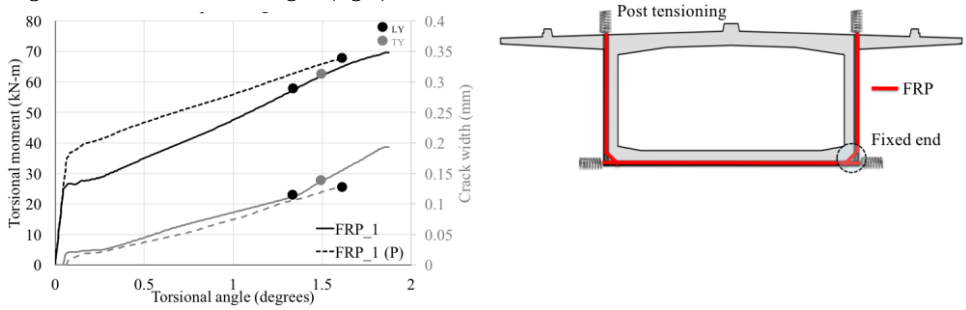

Fig. 7 Results of strengthened beam model FRP_1 with prestress (right); New NSM-CFRP technique for the shear and torsional strengthening of tubular type bridge sections.

5 Conclusions

According to the results obtained from the numerical analysis, the following conclusions can be drawn on the torsional behaviour of thin walled reinforced concrete structures and the strengthening proposals:

- The torsional capacity of the strengthened beams FRP_1, FRP_2, FRP_3 and FRP_4 was 7, 10, 12 and 15% higher than the reference beam, respectively;
- Eventhough the maximum increase in torsional capacity is 15% (θ_t=1.67), it is successful in arresting the crack propagation and in reducing the maximum crack width;
- The increase in longitudinal reinforcement ratio is more effective in increasing the torsional capacity of the beams;
- The variation of E_f corresponds to its effective contribution to the torsional capacity of the beam and controls the yielding of reinforcements;
- The pre-stressed NSM FRP laminates significantly increase the torsional capacity of the beam in serviceability limit state, delaying the yield initiation of steel reinforcemnts and reducing the maximum crack width.

Acknowledgment

The authors acknowledge the support of Marie Curie Initial Training Network under the project "ENDURE" with reference number 607851, funded by the EU programme: FP7-people. The study reported in the paper is a part of ongoing PhD research for the project ENDURE.

References

Al-Mahaidi, Riadh, and Adrian. K Y Hii. 2007. 'Bond Behaviour of CFRP Reinforcement for Torsional Strengthening of Solid and Box-Section RC Beams.' *Composites Part B: Engineering* 38 (5-6): 720–31. doi:10.1016/j.compositesb.2006.06.018.

Baghi, H.; Barros, J.A.O., Ventura-Gouveia, A., "Shear strengthening of reinforced concrete beams with hybrid composite plates", accepted to be published in the Journal of Advances in Structural Engineering, submitted in December 2014.

Breveglieri, Matteo. 2015. 'Shear strengthening of RC beams using embedded through-section technique', PhD Thesis, Ferrara University and Minho University, 2015.

Chalioris, C.E. 2007. 'BEHAVIOURAL MODEL OF FRP STRENGTHENED REINFORCED CONCRETE BEAMS UNDER TORSION.' *Journal of Composites for Construction* 11 (2): 192–200. doi:10.1061/(ASCE)1090-0268(2007)11:2(192).

Chalioris, Constantin E. 2007. 'Analytical Model for the Torsional Behaviour of Reinforced Concrete Beams Retrofitted with FRP Materials.' *Engineering Structures* 29 (12): 3263–76. doi:10.1016/j.engstruct.2007.09.009.

Chalioris, Constantin E., and Chris G. Karayannis. 2009. 'Effectiveness of the Use of Steel Fibres on the Torsional Behaviour of Flanged Concrete Beams.' *Cement and Concrete Composites* 31 (5). Elsevier Ltd: 331–41. doi:10.1016/j.cemconcomp.2009.02.007.

Deifalla, A, and A Ghobarah. 2005. 'Simplified Analysis for Torsionaly Strengthened RC Beams Using FRP.' In *Proceedings of International Symposium on Bond Behaviour of FRP in Structures (BBFS 2005), Hong Kong, December 5-7, 2005*.

Deifalla, A., A. Awad, and M. Elgarhy. 2013. 'Effectiveness of Externally Bonded CFRP Strips for Strengthening Flanged Beams under Torsion: An Experimental Study.' *Engineering Structures* 56. Elsevier Ltd: 2065–75. doi:10.1016/j.engstruct.2013.08.027.

Deifalla, A., and A. Ghobarah. 2010. 'Strengthening RC T-Beams Subjected to Combined Torsion and Shear Using FRP Fabrics: Experimental Study.' *Journal of Composites for Construction* 14 (3): 301–11. doi:10.1061/(ASCE)CC.1943-5614.0000091.

Dias, S. J E, and J. A O Barros. 2013. 'Shear Strengthening of RC Beams with NSM CFRP Laminates: Experimental Research and Analytical Formulation.' *Composite Structures* 99: 477–90. doi:10.1016/j.compstruct.2012.09.026.

EuroCode 2. 2004. 'EN 1992-1-1:2004 - Eurocode 2: Design of Concrete Structures - Part 1-1: General Rules and Rules for Buildings.' *CEN, Brussels*.

Gouveia, António Ventura. 2011. 'Constitutive Models for the Material Nonlinear Analysis of Concrete Structures Including Time-Dependent Effects.' University of Minho, Guimaraes, Portugal.

Hii, Adrian. K Y, and Riadh Al-Mahaidi. 2006. 'An Experimental and Numerical Investigation on Torsional Strengthening of Solid and Box-Section RC Beams Using CFRP Laminates.' *Composite Structures* 75 (1-4): 213–21. doi:10.1016/j.compstruct.2006.04.050.

Jing, Meng, Werasak Raongjant, and Zhongxian Li. 2007. 'Torsional Strengthening of Reinforced Concrete Box Beams Using Carbon Fiber Reinforced Polymer.' *Composite Structures* 78 (2): 264–70. doi:10.1016/j.compstruct.2005.10.017.

Panchacharam, Saravanan, and Abdeldjelil Belarbi. 2002. 'Torsional Behavior of Reinforced Concrete Beams Strengthened with FRP Composites.' In *First FIB Congress on Concrete Structures in 21st Century, Osaka, Japan, October 13-19,2002*, 1–11.

Rezazadeh, Mohammadali, Hadi Baghi, Joaquim Barros, and João Laranjeira. 2015. 'Exploring the Potentialities of a New Type of Cfrp Laminate for the Simultaneous Flexural and Shear Strengthening of Rc Beams : Numerical Research.' In *The 12th International Symposium on Fiber Reinforced Polymers for Reinforced Concrete Structures (FRPRCS-12) & The 5th Asia-Pacific Conference on Fiber Reinforced Polymers in Structures (APFIS-2015) Joint Conference, 14-16 December 2015, Nanjing, China*, 14–16.